

# Separation and Characterization of Acetyl and Non-Acetyl Hemicelluloses of *Arundo donax* by Ammonium Sulfate Precipitation

Feng Peng,<sup>†,‡</sup> Jing Bian,<sup>‡</sup> Pai Peng,<sup>‡</sup> Huan Xiao,<sup>§</sup> Jun-Li Ren,<sup>‡</sup> Feng Xu,<sup>†</sup> and Run-Cang Sun<sup>\*,†,‡</sup>

<sup>†</sup>Institute of Biomass Chemistry and Technology, Beijing Forestry University, Beijing, People's Republic of China

<sup>‡</sup>State Key Laboratory of Pulp and Paper Engineering, South China University of Technology, Guangzhou, People's Republic of China

<sup>§</sup>Business College, Beijing Technology and Business University, Beijing, People's Republic of China.

**ABSTRACT:** Delignified *Arundo donax* was sequentially extracted with DMSO, saturated barium hydroxide, and 1.0 M aqueous NaOH solution. The yields of the soluble fractions were 10.2, 6.7, and 10.0% (w/w), respectively, of the dry *Arundo donax* materials. The DMSO-, Ba(OH)<sub>2</sub>- and NaOH-soluble hemicellulosic fractions were further fractionated into two subfractions by gradient 50% and 80% saturation ammonium sulfate precipitation, respectively. Monosaccharide, molecular weight, FT-IR, and 1D (<sup>1</sup>H and <sup>13</sup>C) and 2D (HSQC) NMR analysis revealed the differences in structural characteristics and physicochemical properties among the subfractions. The subfractions precipitated with 50% saturation ammonium sulfate had lower arabinose/xylose and glucuronic acid/xylose ratios but had higher molecular weight than those of the subfractions precipitated by 80% saturation ammonium sulfate. FT-IR and NMR analysis revealed that the highly acetylated DMSO-soluble hemicellulosic subfraction (H<sub>D50</sub>) could be precipitated with a relatively lower concentration of 50% saturated ammonium sulfate, and thus the gradient ammonium sulfate precipitation technique could discriminate acetyl and non-acetyl hemicelluloses. It was found that the DMSO-soluble subfraction H<sub>D50</sub> precipitated by 50% saturated ammonium sulfate mainly consisted of poorly substituted O-acetyl arabino-4-O-methylglucurono xylan with terminal units of arabinose linked on position 3 of xylose, 4-O-methylglucuronic acid residues linked on position 2 of the xylan bone, and the acetyl groups (degree of acetylation, 37%) linked on position 2 or 3. The DMSO-soluble subfraction H<sub>D80</sub> precipitated by 80% saturated ammonium sulfate was mainly composed of highly substituted arabino-4-O-methylglucurono xylan and β-D-glucan.

**KEYWORDS:** *Arundo donax*, hemicelluloses, gradient ammonium sulfate fractionation, characteristics

## ■ INTRODUCTION

With the depletion of fossil fuel and the concern of environmental protection, the development of sustainable polymers from lignocellulosic biomass is receiving increased attention. The sources of biomass can be divided into two domains. The first domain mainly consists of the organic fraction of municipal wastes and the residual material from forestry and agriculture, such as wood, straw, etc. The second domain is energy crops, such as whole cereal plants, willows, and fodder grasses specifically to generate electricity or produce biofuel.<sup>1</sup> Since the 1970s, biomass crops have attracted increasing interest in energy supplies because they can satisfy a relevant part of the energy demand and at the same time reduce carbon dioxide (CO<sub>2</sub>) emission.<sup>2,3</sup> *Arundo donax* is a fast-growing perennial grass, native to East Asia, and is widespread throughout the Mediterranean area; it has been highlighted as one of the most promising crops in terms of energy production in southern Europe.<sup>4,5</sup> It has been reported that it has an annual production range from 20 to 25 ton/ha per year (dry mass) to 100 ton/ha per year (dry mass) under appropriate plantation conditions.<sup>6</sup> The components (percent, w/w) of *Arundo donax* were cellulose 28–36%, hemicelluloses 20–30%, lignin 16–22%, extractives 7–17%, and ash 3–6% at different morphological regions (internodes, nodes, and foliage) and different stages of maturity.<sup>7</sup> The cellulose, hemicelluloses, and lignin contents of *Arundo donax* are similar

to previous reports for other grass, such as wheat straw<sup>8</sup> and bamboo.<sup>9</sup> Their extractive contents are relatively higher than those of other monocotyledons.<sup>10</sup> Potential applications of *Arundo donax* include the use as a source of fiber for paper,<sup>11</sup> chemical feedstocks, and energy products.<sup>6</sup> To improve its utilization, it is necessary to broaden the knowledge of structural features of its components. A great number of papers have dealt with the cultivation, productivity, and thermal degradation characteristics.<sup>1,2,12</sup> However, only a few papers have reported on the detailed structural characteristics of hemicelluloses and lignin from *Arundo donax*.<sup>13,14</sup>

Hemicelluloses are noncellulosic and short-branched chain heteropolysaccharides consisting of various different sugar units, which are arranged in various proportions and substituents.<sup>15</sup> The average degree of polymerization (DP) of hemicelluloses is in the range of 80–200. Hemicelluloses have gained increasing interest due to their potential as fuel ethanol and other value-added chemicals, such as 5-hydroxymethylfurfural (HMF), furfural, levulinic acid, and xylitol,<sup>16</sup> as viscosity modifiers in food packaging film, as wet strength additives in papermaking, as wound dressings, and as pharmaceutical

**Received:** October 17, 2011

**Revised:** March 23, 2012

**Accepted:** April 5, 2012

**Published:** April 5, 2012

auxiliaries.<sup>17,18</sup> In addition, hemicelluloses have a series of possible medical uses. For example, immunostimulating activities have been reported for arabinoglucuronoxylans from *Echinacea purpurea*.<sup>19</sup> The highly branched, partially *O*-acetylated  $\beta$ -1,4-D-xylan backbone carrying terminal  $\beta$ -D-xylopranosyl units and acidic disaccharide side chains showed strong anticomplementary activity.<sup>20</sup> The water-soluble arabinoglucuronoxylans from corn cobs exhibited significant immunostimulatory effects in vitro rat thymocyte test, which was comparable to those of the commercial immunomodulator Zymosan, a fungal  $\beta$ -glucan.<sup>21</sup>

Hemicelluloses are usually associated with various other cell-wall components such as cellulose, cell-wall proteins, lignin, and other phenolic compounds by covalent, hydrogen bonding, and ionic and hydrophobic interactions.<sup>22</sup> In the conventional kraft pulping process, most of the hemicelluloses from wood are degraded into oligomers or mono sugars and dissolved in black liquor along with dissolved lignin and the pulping chemicals (inorganic substances). In addition, during the production of ethanol, the removal of hemicelluloses is desired to improve the accessibility of cellulosic material to hydrolytic enzymes. Therefore, efficient utilization of the biomass components by pre-extraction and isolation of hemicelluloses will increase revenue streams for the lignocellulosic biorefinery and help to maximize the utilization of biomass in the production of fuels, chemicals, and materials. The isolation of hemicelluloses from the raw material or holocellulose can be performed by organic solvent (dimethyl sulfoxide, DMSO) or alkaline aqueous solution (NaOH and KOH) extractions. A part of the hemicelluloses can be extracted with DMSO, and the advantage is that no cleavages of chemical linkages take place, which aids in the study of their structure. Successive alkali treatments with increasing concentrations avoid unnecessary exposure of hemicellulosic materials to a high concentration of alkali and yield polysaccharides having different structural features.<sup>23</sup>

Hemicelluloses generally display a high degree of polydispersity in their molecular size and chemical structure and exhibit variations in proportions of sugar constituents, linkage type, functional groups (i.e., OH groups, acetoxy groups, carboxyl groups, methoxyl groups, etc.), or degree and arrangement of branching. Due to their different chemical and molecular structures, hemicelluloses represent a different type of polysaccharide that behaves differently from cellulose and starch. Relatively small differences in the structure of polysaccharides may give rise to substantial variations in their physicochemical properties and applications. For example, non-acetyl hemicelluloses with one or two free hydroxyl groups are hydrophilic, and acetyl hemicelluloses are usually hydrophobic.<sup>24</sup> Acetylation of the hydroxyl groups of hemicelluloses is one approach toward increasing the water resistances of hemicelluloses.<sup>25</sup> In addition, acetyl hemicelluloses have higher thermal stability than non-acetyl hemicelluloses.<sup>24,25</sup> Therefore, it is sometimes necessary, when examining their molecular structures or structure–property relationships, to fractionate them into structurally more homogeneous material. In recent years, much attention has been paid to developing effective isolation and purification methods to obtain homogeneous hemicelluloses with both high purity and yield. In our previous studies, several fractionation techniques, such as graded ethanol precipitation,<sup>26</sup> iodine-complex precipitation,<sup>27</sup> and anion-exchange chromatography<sup>28</sup> have been employed to obtain homogeneous fractions. Graded ethanol precipitation and anion-exchange chromatography could be used for fractiona-

tion of hemicelluloses having a degree of branching and molecular weight different from those of lignocellulosic materials.<sup>26,28</sup> Iodine-complex precipitation could discriminate between linear and branched polysaccharides.<sup>27</sup> Salting-out procedures, such as ammonium sulfate precipitation, commonly utilized in the isolation and fractionation of proteins,<sup>29</sup> have received less attention in the area of isolation and fractionation of polysaccharides. In the current work, the hemicellulosic fractions were prepared by stepwise extraction of *Arundo donax* samples with DMSO, saturated Ba(OH)<sub>2</sub>, and aqueous 1.0 M NaOH, followed by subfractionation through precipitation with gradient ammonium sulfate. Moreover, the structural characterization of each subfraction was investigated by high-performance anion exchange chromatography (HPAEC), Fourier transform infrared spectra (FT-IR), gel permeation chromatography (GPC), and nuclear magnetic resonance (NMR) spectra.

## MATERIALS AND METHODS

**Materials.** *Arundo donax* was harvested in January 2011 in Sichuan Province, People's Republic of China. After removal of leaves, the trunks were chipped into small pieces. The chips were dried in sunlight and then ground to pass a 0.8 mm screen. After being further dried at 60 °C for 16 h, the powder was dewaxed with 2/1 (v/v) toluene/ethanol in a Soxhlet apparatus for 6 h. The dewaxed sample was further dried in a cabinet oven with air circulation at 60 °C for 16 h. The components (percent, w/w) of the *Arundo donax* were holocellulose 66.1%, pentosans 25.4%, Klason lignin 19.9%, extractives 1.5%, and ash 3.9%, which were determined according to Tappi standards (Tappi 2002) for measuring the chemical composition. All standard chemicals were analytical grade, purchased from Sigma Chemical Company (Beijing).

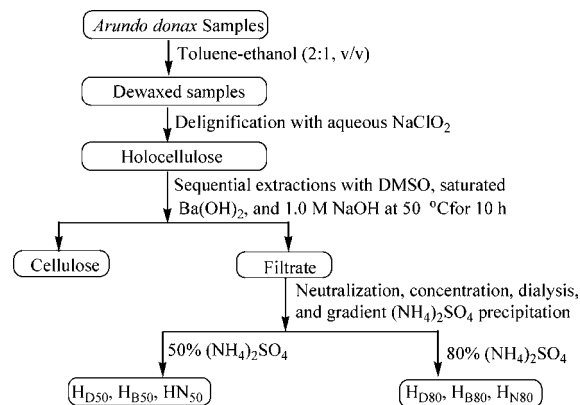


**Figure 1.** Scheme for fractional isolation of hemicelluloses from *Arundo donax*.

**Extraction and Fractionation.** The fractional isolation of hemicelluloses from *Arundo donax* is illustrated in Figure 1. The dewaxed powder was delignified with 6% sodium chlorite at pH 3.6–3.8, adjusted with 10% acetic acid, at 75 °C for 2 h. The residue, holocellulose, was subsequently washed with distilled water and dried at 60 °C for 16 h. Then the holocellulose (25.0 g) was successively extracted by dimethyl sulfoxide (DMSO), saturated Ba(OH)<sub>2</sub>, and 1.0 M aqueous NaOH with a solid to liquid ratio of 1/25 (g mL<sup>-1</sup>) at 80 °C for 10 h under stirring. After the indicated period of treatment, the insoluble residues were collected by filtration, washed with distilled water until the pH of the filtrates was neutral, and then dried at 60 °C for 16 h. The filtrate obtained by DMSO treatment was concentrated to about 50 mL and then mixed with three volumes of ethanol. The precipitate was then redissolved in water, ammonium sulfate was

Table 1. Yield and Composition of Hemicellulosic Subfractions from *Arundo donax*

subfraction <sup>a</sup>	yield <sup>b</sup> (%)	molar composition <sup>c</sup> (mol %)					molar ratio	
		Ara	Gal	Glc	Xyl	GlcA	GlcA/Xyl	Ara/Xyl
H <sub>D50</sub>	8.13	4.91	0.19	4.98	87.27	2.65	0.03	0.06
H <sub>D80</sub>	1.15	6.53	5.22	17.03	60.15	11.08	0.18	0.11
H <sub>B50</sub>	3.80	9.60	0.83	3.16	78.60	7.81	0.10	0.12
H <sub>B80</sub>	1.39	15.82	3.68	6.45	61.33	12.72	0.21	0.25
H <sub>N50</sub>	6.17	8.11	0.07	0.48	86.49	4.84	0.06	0.09
H <sub>N80</sub>	2.15	18.96	11.80	10.11	49.79	9.34	0.19	0.38

<sup>a</sup>H<sub>D50</sub> and H<sub>D80</sub>, H<sub>B50</sub> and H<sub>B80</sub>, and H<sub>N50</sub> and H<sub>N80</sub> represent the subfractions precipitated at 50% and 80% (NH<sub>4</sub>)<sub>2</sub>SO<sub>4</sub> from DMSO-, Ba(OH)<sub>2</sub>-, and NaOH-soluble hemicelluloses, respectively. <sup>b</sup>Based on dry starting materials (w/w). <sup>c</sup>Expressed in relative molar percentages.

added slowly up to 50% saturation, and the solution was allowed to stand overnight at 25 °C. The precipitated hemicelluloses were collected by centrifugation (3500 g, 15 min), redissolved in distilled H<sub>2</sub>O, and dialyzed until free of (NH<sub>4</sub>)<sub>2</sub>SO<sub>4</sub>, freeze-dried, and designated as H<sub>D50</sub>. Then the saturation level of (NH<sub>4</sub>)<sub>2</sub>SO<sub>4</sub> in the remaining filtrate was subsequently adjusted to 80%. The corresponding precipitated hemicelluloses were labeled as H<sub>D80</sub>. The filtrates obtained by the treatment of saturated Ba(OH)<sub>2</sub> and 1.0 M NaOH were adjusted to pH at 6.0 with 6.0 M HCl, concentrated, and dialyzed until free of BaCl<sub>2</sub> or NaCl to give saturated Ba(OH)<sub>2</sub> and 1.0 M NaOH extracts, which were further fractionated by ammonium sulfate precipitation in a manner similar to that mentioned above. Four subfractions were obtained from each extract: H<sub>B50</sub>, H<sub>N50</sub>, H<sub>B80</sub>, and H<sub>N80</sub>. H<sub>B50</sub> and H<sub>N50</sub> were obtained by precipitation with 50% saturated ammonium sulfate, and hemicellulosic subfractions (H<sub>B80</sub> and H<sub>N80</sub>) were obtained by precipitating with 80% saturated ammonium sulfate from saturated Ba(OH)<sub>2</sub> and NaOH extracts, respectively.

**Analytical Methods.** The composition of neutral sugars and uronic acids and the molecular weights of the hemicellulosic samples were determined according to the literature.<sup>27</sup> FT-IR experiments were conducted using a Thermo Scientific Nicolet iN 10 FT-IR Microscopy (Thermo Nicolet Corp., Madison, WI) equipped with a liquid nitrogen cooled MCT detector. Dried samples were ground and pelletized using BaF<sub>2</sub>, and their spectra were recorded from 4000 to 650 cm<sup>-1</sup> at a resolution of 4 cm<sup>-1</sup> and 128 scans per sample. The solution-state <sup>1</sup>H NMR spectra were recorded on a Bruker NMR spectrometer at 400 MHz using 15 mg of hemicelluloses in 1.0 mL of D<sub>2</sub>O. The chemical shifts reported were calibrated relative to the signals from D<sub>2</sub>O, used as an internal standard, at 4.7 ppm for the <sup>1</sup>H NMR spectra. The degree of acetylation (DS<sub>AC</sub>) was determined from the relative intensities of signals of the acetyl group at 2.1 ppm and those of all carbohydrate signals in <sup>1</sup>H NMR spectra. The following equation was used:

$$DS_{AC} = \frac{(\text{sum on integrals for acetyl groups at 2.1 ppm})/3}{(\text{sum of integrals for carbohydrate signals at 3.0–5.5 ppm})/6}$$

The <sup>13</sup>C NMR spectra were recorded at 25 °C after 30 000 scans. The sample (80 mg) was dissolved in 1.0 mL of D<sub>2</sub>O (99.8% D) overnight at room temperature. Chemical shifts ( $\delta$ ) were expressed relative to the resonance of Me<sub>4</sub>Si ( $\delta$  0). A 30° pulse flipping angle, a 3.9  $\mu$ s pulse width, and a 0.85 s delay time between scans were used. The proton-detected heteronuclear single quantum correlation (HSQC) spectra were acquired by the HSQCGE experiment mode, over a  $t_1$  spectral width of 10 000 Hz and a  $t_2$  width of 1800 Hz, and the acquired time (AQ) was 0.1163 s. The number of scan (NS) was 32. The delay between transients was 2.6 s, and the delay for polarization transfer was set to correspond to an estimated average <sup>1</sup>H–<sup>13</sup>C coupling constant of 150 Hz. Data processing was performed using standard Bruker Topspin-NMR software.

## RESULTS AND DISCUSSION

**Yield and Composition.** In plant cell walls, there are large amounts of hemicelluloses with a wide variation in content and chemical structure. Hemicelluloses generally consist of several populations of polysaccharide molecules which vary in structural characteristics. In general, one-step dilute alkali treatment extracted only part of the hemicelluloses from both holocellulose and lignified materials. Successive treatments with neutral solvent or alkali of initially low and then high concentration avoid unnecessary exposure of hemicellulosic material to alkali that is more concentrated than that required for the extraction.<sup>30,31</sup> In this case, sequential extractions of hemicelluloses with DMSO, saturated Ba(OH)<sub>2</sub>, and 1.0 M NaOH at 50 °C were performed. The sequential treatments solubilized 10.2, 6.7, and 10.0% of the hemicelluloses (percent dry matter), respectively. In addition, stepwise addition of ammonium sulfate to the solution of the three hemicelluloses resulted in six subfractions. The yield and composition of each subfraction are presented in Table 1. On the basis of the total amount of dry material recovered, 8.1, 3.8, and 6.2% polymers were precipitated at 50% saturation (NH<sub>4</sub>)<sub>2</sub>SO<sub>4</sub>, accounting for 79.5, 56.4, and 61.6% of DMSO, saturated Ba(OH)<sub>2</sub>, and 1.0 M NaOH soluble hemicelluloses, respectively. Three other subfractions were recovered after adjustment of the saturation level of (NH<sub>4</sub>)<sub>2</sub>SO<sub>4</sub> to 80%, and their yields were 11.2, 20.7, and 21.5% of DMSO, saturated Ba(OH)<sub>2</sub>, and 1.0 M NaOH soluble hemicelluloses, respectively. Taken together, 90.7%, 77.1%, and 83.1% of DMSO, saturated Ba(OH)<sub>2</sub>, and 1.0 M NaOH soluble hemicelluloses were recovered by 50% and 80% saturated (NH<sub>4</sub>)<sub>2</sub>SO<sub>4</sub> precipitation, respectively, indicating that small amounts of hemicelluloses, mainly degraded oligosaccharides, were not recovered.

The sugar components of the six subfractions are presented in Table 1. All the hemicellulosic subfractions were composed mainly of xylose (49.8–87.3%), arabinose (4.9–19.0%), and glucuronic acid (4.8–12.7%). Small amounts of glucose and galactose were also detected. The data above suggested that a substantial proportion of the polysaccharide in the cell walls of *Arundo donax* consists of glucuronoarabinoxylans, which were also found in other grasses, such as bamboo,<sup>32</sup> Vetiver grass,<sup>33</sup> etc. The presence of glucose (3.2–17.0%) probably originated from  $\beta$ -D-glucan, which was a group of polysaccharides found in the cell wall of gramine, including grasses and cereals, and need to be further characterized.<sup>34</sup>

It should be noted that in H<sub>D50</sub> and H<sub>D80</sub> obtained from the DMSO-soluble hemicelluloses, xylose decreased from 87.3% (H<sub>D50</sub>) to 60.2% (H<sub>D80</sub>), whereas arabinose increased from 4.9% to 6.5%, and glucuronic acid (GlcA) from 2.7% to 11.1%. The ratios of arabinose to xylose (Ara/Xyl) and glucuronic acid

to xylose (Glc pA/Xyl) are indicative of the degree of linearity or branching of hemicelluloses.<sup>35</sup> The ratios of Ara/Xyl and Glc pA/Xyl increased from 0.06 to 0.11 and from 0.06 to 0.18, respectively, with increasing concentrations of saturated ammonium sulfate from 50% to 80%. Similar results were also observed for other four hemicellulosic subfractions ( $H_{B50}$ ,  $H_{B80}$ ,  $H_{N50}$ , and  $H_{N80}$ ) obtained from saturated  $Ba(OH)_2$ - and NaOH-soluble hemicelluloses, respectively. These results suggested that the hemicellulosic subfractions precipitating at the lower saturation level of ammonium sulfate (50%) had a lesser substituted xylan backbone as compared with those subfractions at a higher salt concentration (80%), which were consistent with the results found for arabinoxylans of wheat endosperm<sup>36</sup> and wheat flour<sup>37</sup> and glucuronoarabinoxylans of sugar cane bagasse<sup>26</sup> by graded ethanol or ammonium sulfate precipitation techniques. The exact mechanism of polysaccharide fractionation with  $(NH_4)_2SO_4$  is not yet fully known, but the results of the present study indicated that the less branched hemicellulose backbones were more likely to aggregate, force out of the solution, and precipitate at relatively low levels of  $(NH_4)_2SO_4$  saturation.

**Molecular Weight.** Differences in molecular weights among the six subfractions were revealed by gel permeation chromatography (GPC). The molecular weight data was based on the amount of soluble material passing through the column, which was denoted as GPC recovery. The values of the weight-average ( $M_w$ ) and number-average ( $M_n$ ) molecular weights and polydispersity ( $M_w/M_n$ ) of the six hemicellulosic polymers are given in Table 2. As can be seen, the  $M_w$  values of

**Table 2. Weight-Average ( $M_w$ ) and Number-Average ( $M_n$ ) Molecular Weights (g/mol) and Polydispersity ( $M_w/M_n$ ) of the Hemicellulosic Subfractions**

	hemicellulosic subfractions <sup>a</sup>					
	$H_{D50}$	$H_{D80}$	$H_{B50}$	$H_{B80}$	$H_{N50}$	$H_{N80}$
$M_w$	38 100	18 350	28 650	13 570	19 190	11 560
$M_n$	12 400	3 220	6 820	2 220	3 990	1 650
$M_w/M_n$	3.1	5.7	4.2	6.1	4.8	7.0

<sup>a</sup>Corresponding to the hemicellulosic subfractions in Table 1.

hemicelluloses followed this order: DMSO-soluble hemicelluloses ( $H_{D50}$  and  $H_{D80}$ ) > saturated  $Ba(OH)_2$ -soluble hemicelluloses ( $H_{B50}$  and  $H_{B80}$ ) > 1.0 M KOH-soluble hemicelluloses ( $H_{N50}$  and  $H_{N80}$ ). This indicated that on treatment with the neutral solvent (DMSO), the hemicelluloses were not degraded, but the treatment of 1.0 M aqueous NaOH resulted in a slight degradation of the macromolecular structure of hemicelluloses. In addition, for DMSO-soluble hemicellulosic subfractions ( $H_{D50}$  and  $H_{D80}$ ),  $H_{D50}$  obtained by precipitation with 50% saturated ammonium sulfate had a higher  $M_w$  value of 38 100 g mol<sup>-1</sup> in comparison to that for  $H_{D80}$  ( $M_w = 18 350$  g mol<sup>-1</sup>) precipitated with 80% saturated ammonium sulfate. These trends were also observed in other four subfractions ( $H_{B50}$  and  $H_{B80}$ ,  $H_{N50}$  and  $H_{N80}$ ), which suggested that subfractions exhibiting higher molecular weight were precipitated with a concentration of saturated ammonium sulfate lower than those precipitated with the higher concentration of  $(NH_4)_2SO_4$ . On the basis of this observation and the Glc pA/Xyl and Ara/Xyl ratios, it could be concluded that the less branched hemicelluloses with a high molecular weight were precipitated in lower ammonium sulfate percentages, while with increasing ammonium sulfate concen-

trations, more branched hemicelluloses with low molecular weights were obtained; this is in good agreement with the results of other studies on alkali-extracted arabinoxylans of wheat flour and glucuronoarabinoxylans of sugar cane bagasse.<sup>26,38,39</sup> However, Hoffmann et al. did not observe such a relationship, in which the highly branched arabinoxylan fractions with a high Ara/Xyl ratio had higher  $M_w$  values than those of less branched counterparts.<sup>36</sup> It was also found that the linear hemicelluloses of hardwood (*Populus gansuensis*) had a higher molecular weight than the branched hemicelluloses.<sup>27</sup> These differences in molecular weights are probably due to the differences in their botanical origin. Furthermore, the polydispersity indexes of six subfractions are also shown in Table 2. In comparison to those of the hemicellulosic subfractions precipitated by 50% saturated ammonium sulfate, with polydispersity indexes of 3.1, 4.2, and 4.8, the hemicellulosic subfractions  $H_{D80}$ ,  $H_{B80}$ , and  $H_{N80}$  had more broad molecular weight distribution, corresponding to polydispersity indexes of 5.1, 6.7, and 7.0, respectively. The high polydispersity indexes probably reflected that the hemicellulosic subfractions precipitated by 80% saturated ammonium sulfate contained several kinds of polysaccharides, which is in agreement with the relatively high content of glucose and galactose in sugar composition analysis (Table 1).

**FT-IR Spectra.** FT-IR spectroscopy has shown to be a useful tool in monitoring structural changes of biopolymers.<sup>40</sup> The FT-IR spectra of DMSO-soluble subfractions  $H_{D50}$  (spectrum a) and  $H_{D80}$  (spectrum b) precipitated by 50% and 80% saturated ammonium sulfate are shown in Figure 2. The IR spectra show a strong hydrogen-bonded O–H stretching absorption around 3427 cm<sup>-1</sup> and prominent C–H stretching absorptions at 2921 and 2850 cm<sup>-1</sup>. The sharp signal at 1737 cm<sup>-1</sup>, attributed to C=O stretching of carbonyl and acetyl groups in the hemicelluloses,<sup>41</sup> is present in  $H_{D50}$  (spectrum a) obtained at 50% saturated ammonium sulfate, which indicates that on treatment with dimethyl sulfoxide, the most common neutral (nondestructive) solvent, the hemicelluloses can be extracted without cleaving the acetyl ester groups. The acetyl group is believed to be mostly associated either with xylose or uronic acid residues of hemicelluloses and is easily cleaved by alkali.<sup>42</sup> However, the absence of a signal at 1737 cm<sup>-1</sup> in  $H_{D80}$  (spectrum b) implied that the graded ammonium sulfate technique can discriminate acetyl and non-acetyl hemicelluloses. Evidently, the major bands at 1037 and 1093 cm<sup>-1</sup> are assigned to the C–OH bending mode.<sup>40</sup> The small band at 1162 cm<sup>-1</sup> (spectrum a, data not shown) is assigned to the C–O stretching in C–O–C glycosidic linkages, and the contribution of C–OH bending from arabinoxylans and the variation of the signal intensity reflect the degree of substitution by arabinose residues.<sup>41</sup> The absorbance at 896 cm<sup>-1</sup> (spectrum a), the carbohydrate C<sub>1</sub>–H deformation and ring-stretching frequency, is characteristic of dominant  $\beta$ -glycosidic linkages between the sugar units in the subfractions. The signals at 857 and 767 cm<sup>-1</sup> are indicative of  $\alpha$ -glycosidic linkages, which indicate that the arabinose, glucose, and glucuronic acid are probably linked by  $\alpha$ -glycosidic linkages.<sup>43</sup> In addition, two bands at 1625 and 1411 cm<sup>-1</sup> are assigned to the –COO<sup>-</sup> antisymmetric and symmetric stretching of glucuronic acid or glucuronic acid carboxylate, respectively.<sup>44,45</sup> The remaining bands at 1235 and 1378 cm<sup>-1</sup> represent OH in-plane and CH bending vibrations, respectively.<sup>45</sup>

Figure 3 illustrates the FT-IR spectra of saturated  $Ba(OH)_2$ -soluble hemicellulosic subfractions  $H_{B50}$  (spectrum a) and  $H_{B80}$

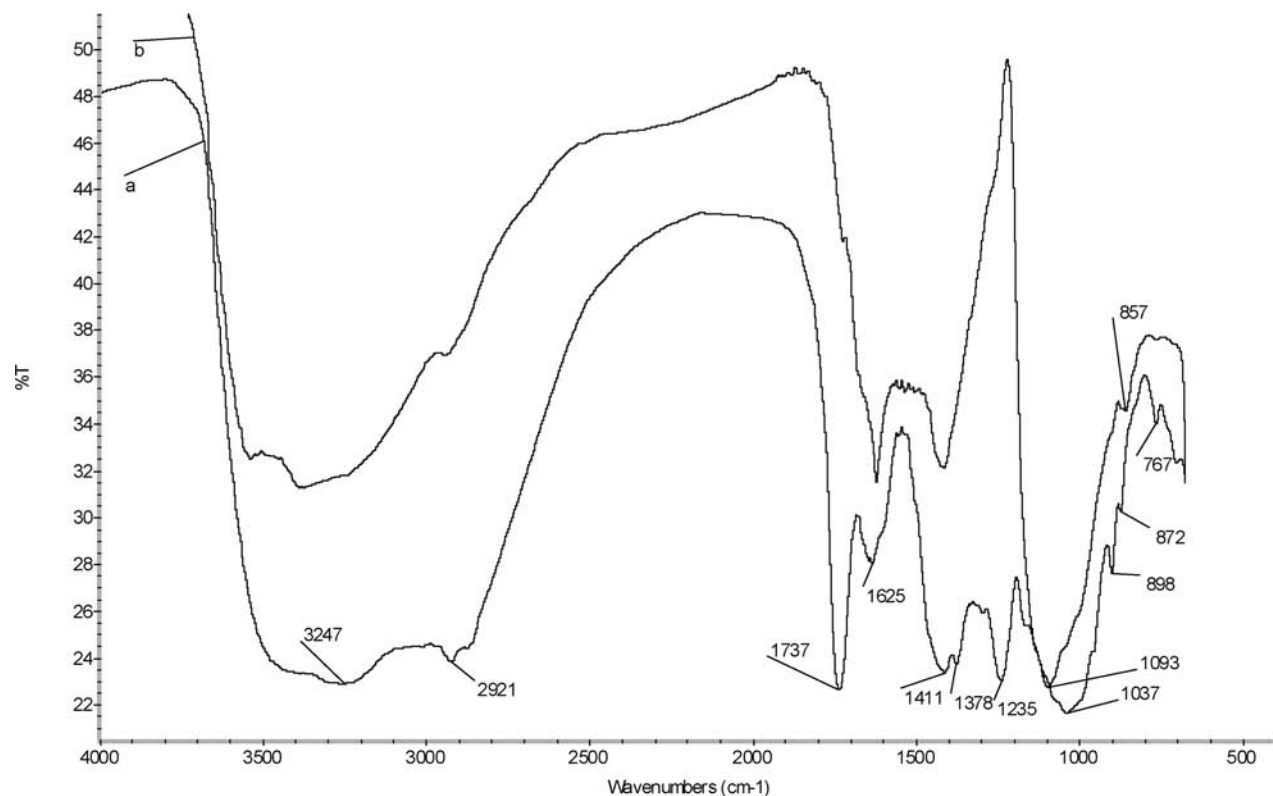


**Figure 2.** FT-IR spectra of DMSO-soluble hemicellulosic subfractions  $H_{D50}$  (spectrum a) and  $H_{D80}$  (spectrum b).

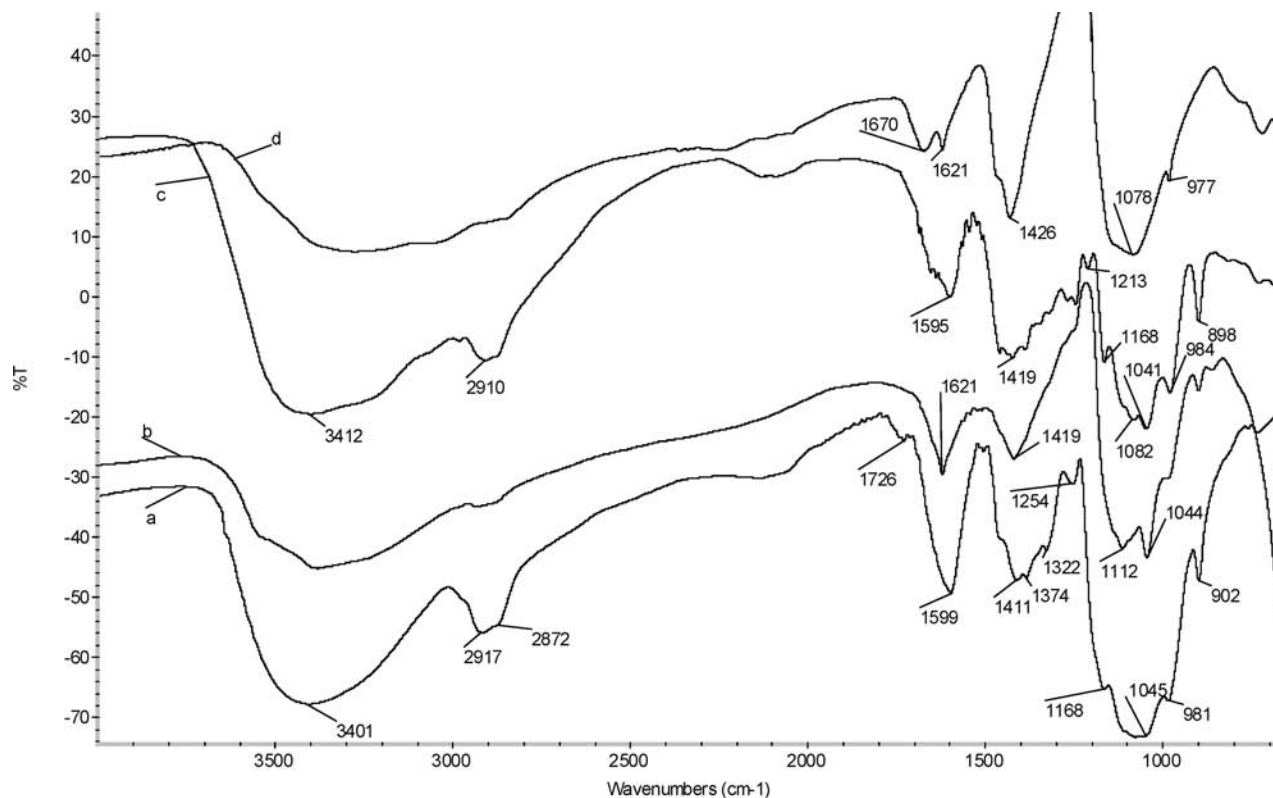


**Figure 3.** FT-IR spectra of  $Ba(OH)_2$ -soluble hemicellulosic subfractions  $H_{B50}$  (spectrum a) and  $H_{B80}$  (spectrum b) and NaOH-soluble hemicellulosic subfractions  $H_{N50}$  (spectrum c) and  $H_{N80}$  (spectrum d).

(spectrum b) precipitated by 50% and 80% saturated ammonium sulfate. Typical signals of hemicelluloses were observed at 3401, 2917, 2872, 1599, 1411, 1168, 1044, and 902

$cm^{-1}$ . In comparison with the spectrum of DMSO-soluble subfraction  $H_{D50}$ , the much weaker band at 1726  $cm^{-1}$  (spectrum a,  $H_{B50}$ ) in Figure 3 demonstrated that the

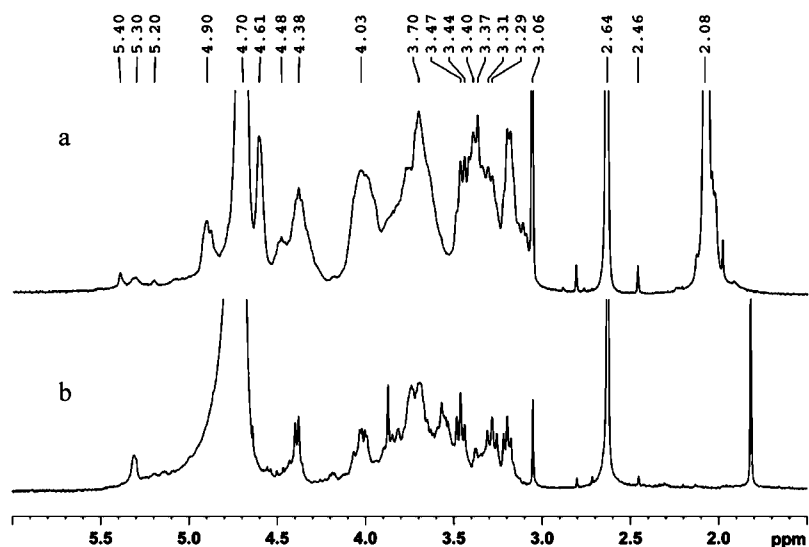


Figure 4.  $^1\text{H}$  NMR spectra of hemicellulosic subfractions  $\text{H}_{\text{D50}}$  (spectrum a) and  $\text{H}_{\text{D80}}$  (spectrum b).

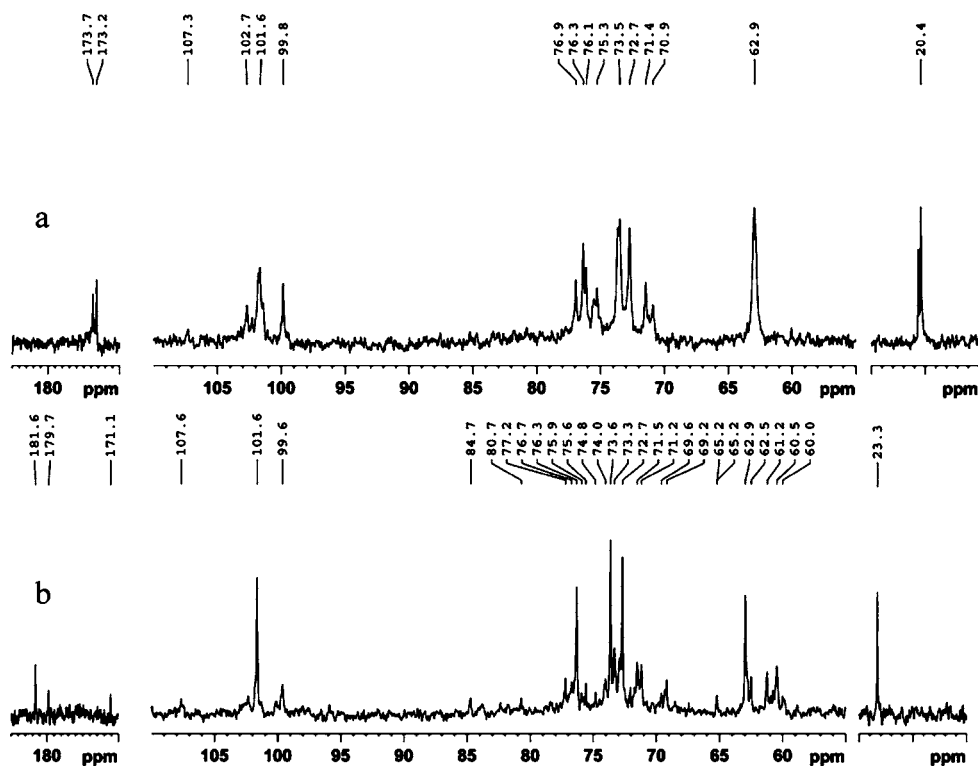


Figure 5.  $^{13}\text{C}$  NMR spectra of hemicellulosic subfractions  $\text{H}_{\text{D50}}$  (spectrum a) and  $\text{H}_{\text{D80}}$  (spectrum b).

treatment with saturated  $\text{Ba}(\text{OH})_2$  substantially cleaved the acetyl group of hemicelluloses. In addition, the band at  $1726\text{ cm}^{-1}$  is absent in the subfraction  $\text{H}_{\text{D80}}$  (spectrum b) but is present in  $\text{H}_{\text{D50}}$  (spectrum a), which is in good agreement with the result of FT-IR spectra of DMSO-soluble hemicellulosic subfractions in Figure 2. The occurrence of a small peak in spectrum a at  $1505\text{ cm}^{-1}$  originates from aromatic skeletal vibrations in the associated lignin, indicating that  $\text{H}_{\text{D50}}$  is contaminated with minimal amounts of bound lignin.<sup>46</sup> The FT-IR spectra of aqueous  $\text{NaOH}$ -soluble hemicellulosic subfractions  $\text{H}_{\text{N50}}$  (spectrum c) and  $\text{H}_{\text{N80}}$  (spectrum d) are shown in Figure 3. As can be seen, the disappearance of signal around  $1730\text{ cm}^{-1}$  (spectrum a) revealed that the alkaline

extraction under the conditions used completely saponified ester bonds.

**NMR Spectra.** DMSO is expected to extract hemicelluloses without degradation, in contrast to the case for alkaline extractions, which will cause de-*O*-acetylation. For this reason, structural analysis was only performed on the DMSO hemicellulosic subfractions ( $\text{H}_{\text{D50}}$  and  $\text{H}_{\text{D80}}$ ). 1D ( $^1\text{H}$  and  $^{13}\text{C}$ ) and 2D (HSQC) NMR spectra of  $\text{H}_{\text{D50}}$  and  $\text{H}_{\text{D80}}$  were collected in order to elucidate the structural features.  $^1\text{H}$  NMR spectra of  $\text{H}_{\text{D50}}$  (spectrum a) and  $\text{H}_{\text{D80}}$  (spectrum b) are shown in Figure 4. As can be seen, the relevant signals occurred in two regions: namely, the anomeric region ( $4.3\text{--}4.9\text{ ppm}$  for  $\beta$ -anomers and  $4.9\text{--}5.6\text{ ppm}$  for  $\alpha$ -anomers) and the ring proton

region (4.3–3.0 ppm). From the anomeric region, the spectra of the two subfractions revealed that the DMSO-soluble hemicelluloses are mainly composed of three populations. The signals at 4.38 ppm are assigned to the anomeric protons of (1→4)-linked  $\beta$ -D-Xylp. The signal at 5.4 ppm originates from anomeric protons of terminal Araf linked to O-3 of Xylp.<sup>47</sup> An anomeric proton at 5.3 ppm is characteristic of 4-O-methylglucuronic acid attached via  $\alpha$ -(1→2) linkage to xylose.<sup>48</sup> A strong resonance at 5.3 ppm found in H<sub>D80</sub> (spectrum b) precipitated by 80% saturated ammonium sulfate indicated that a majority of the branching sites were represented by singly substituted Xylp. These results were in agreement with the results of sugar analysis (Table 1). The signal at 2.1 ppm indicated that the hemicellulosic subfraction H<sub>D50</sub> precipitated by 50% saturated ammonium sulfate was highly acetylated. The degree of acetyl substitution (DS<sub>AC</sub>) of the hemicellulosic subfraction H<sub>D50</sub> was 0.37, which was determined by integration of the signals of acetyl groups at 2.1 ppm and those of all carbohydrate signals.<sup>49</sup> However, the signal at 2.08 ppm was absent in the subfraction H<sub>D80</sub> (Figure 4b), which suggested that the highly acetylated hemicelluloses were precipitated at the relatively lower concentration of saturated ammonium sulfate, corresponding to the results obtained by FT-IR. Obviously, a strong signal at 4.7 ppm originated from the residual solvent (HDO). At 2.6 ppm there was an intense singlet that is assigned to the protons in dimethyl sulfoxide, which originates from the residual DMSO as extractant in the hemicellulosic subfractions.<sup>50</sup>

The <sup>13</sup>C NMR spectra of H<sub>D50</sub> (spectrum a) and H<sub>D80</sub> (spectrum b) exhibit five main signals in Figure 5, one in the anomeric region and four in the skeletal regions for xylose moieties, at 101.6 (C-1), 76.3 (C-4), 73.5 (C-3), 72.7 (C-2), and 62.9 (C-5) ppm, resonances of low intensity for arabinose residues at 107.3 (C-1), 84.7 (C-4), 80.4 (C-2), and 60.5 (C-5) ppm, and small signals for 4-O-methylglucuronic acid residues at 179.7 (C-6), 99.8 (C-1), and 59.9 (–OCH<sub>3</sub>) ppm. However, no signals at 179.7 ppm were detected in Figure 5a, which is probably due to the low amount of 4-O-methylglucuronic acid residues in H<sub>D50</sub>. In addition, two signals at the lowest field of 173.2 and 173.7 (C=O) ppm and a high-field resonance at 20.4 (CH<sub>3</sub>) ppm (Figure 5a) indicated the presence of O-acetyl groups in the hemicellulosic subfraction (H<sub>D50</sub>), but these signals for O-acetyl groups were absent in Figure 5b, which is in accord with the results of FT-IR and <sup>1</sup>H NMR.

The HSQC spectra of H<sub>D50</sub> (spectrum a) and H<sub>D80</sub> (spectrum b) are shown in Figure 6, and the chemical shift assignments are given in Table 3. The anomeric region in the HSQC spectrum is <sup>1</sup>H 4.4–5.5 ppm/<sup>13</sup>C 90–110 ppm, while the O-acetylated xylose region is <sup>1</sup>H 4.5–5.5 ppm/<sup>13</sup>C 70–80 ppm. As can be seen from Figure 6a (H<sub>D50</sub>), the marked <sup>1</sup>H/<sup>13</sup>C cross peaks at 4.38/101.6, 5.4/107.3, and 5.32/99.8 ppm confirmed the structural unit of the (1→4)- $\beta$ -D-xylan backbone and Araf residues at O-3, 4-O-Me- $\alpha$ -D-GlcpA units at position O-2. The cross peaks at 4.61/100.0 and 4.90/74.9 ppm are attributed to H-1/C-1 and H-2/C-2 atoms as a result of acetylation at position 2 of 1,4-linked  $\beta$ -Xylp residues. Similarly, the cross peaks at 4.48/101.5 and 4.61/73.2 ppm are due to H-1/C-1 and H-3/C-3 atoms of acetyl 1,4-linked  $\beta$ -Xylp units, which are substituted at position 3 by acetyl groups.<sup>49</sup> The 2D integrals of H-2/C-2 and H-3/C-3 cross peaks indicated that O-acetyl groups at C-2 and C-3 are in 1/1.8 mol proportion. It is difficult to determine the distribution of O-2 and O-3 acetyl groups on the xylose chain. On the basis of the NMR analysis, it

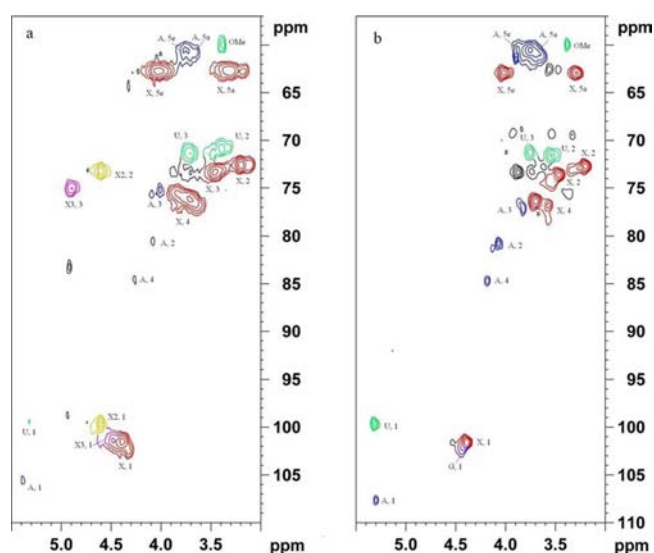


**Figure 6.** HSQC spectra of hemicellulosic subfractions H<sub>D50</sub> (spectrum a) and H<sub>D80</sub> (spectrum b). Designations are follows: X, Xylp; A, Araf; U, 4-O-Me- $\alpha$ -GlcpA; X2, 2-O-acetylated Xylp; X3, 3-O-acetylated Xylp; G, Glcp.

can be concluded that the subfraction H<sub>D50</sub> mainly consists of O-acetyl arabino-4-O-methylglucuronoxylan with the terminal units of arabinose linked on position 3 of xylan, 4-O-methylglucuronic acid residues linked on position 2 of the xylan bone, and acetyl groups linked on position 2 or 3.

As can be seen from Figure 6b and Table 3, the HSQC NMR analysis revealed three important groups: Araf residues, 4-O-Me- $\alpha$ -D-GlcpA-(1→2) units, and (1→4)- $\beta$ -D-Xylp. In addition, a low amount of  $\beta$ -D-glucans (103.3/4.55 ppm) was also observed.<sup>51</sup> Other signals of  $\beta$ -D-glucans are overlapped with those of xylan-type hemicelluloses. The reason for the low intensity of signals from  $\beta$ -D-glucans was probably due to the low solubility in D<sub>2</sub>O at ambient temperature (20 °C).<sup>52</sup> Some acetate was detected at 23.3/1.82 ppm in the H<sub>D80</sub> NMR spectrum (data not shown), and it was unclear whether this originated from the liberation of O-acetyl groups.<sup>49</sup> Therefore, it was concluded that H<sub>D80</sub> was mainly composed of arabino-4-O-methylglucurono xylan and  $\beta$ -D-glucan.

## CONCLUSIONS

The present study was aimed at obtaining detailed structural characteristics of hemicelluloses extracted successively with dimethyl sulfoxide (DMSO), saturated Ba(OH)<sub>2</sub>, and 1.0 M aqueous NaOH from *Arundo donax* and fractionated with the gradient ammonium sulfate technique. The results revealed that *Arundo donax* hemicelluloses had considerable heterogeneity, varying in sugar composition, molecular weight, and structural features. The sugar analysis indicated that the hemicellulosic subfractions precipitating at the lower saturation level of ammonium sulfate (50%) were lesser substituted hemicelluloses as compared with those subfractions obtained at a higher salt concentration (80%). Substantial differences in molecular weight were also found. The DMSO-soluble hemicelluloses had a higher molecular weight, whereas the 1.0 M NaOH-soluble hemicelluloses had a relatively lower molecular weight. In addition, the hemicellulosic subfractions exhibiting higher molecular weight could be precipitated at the lower concentration of saturated ammonium sulfate. In other words, with increasing ammonium sulfate concentrations, the

Table 3. <sup>1</sup>H and <sup>13</sup>C Chemical Shift (ppm) Assignments for Hemicellulosic Subfractions H<sub>D50</sub> and H<sub>D80</sub>

sugar residue	chem shift (ppm) H/C							
	1	2	3	4	Sax <sup>a</sup>	Seq <sup>b</sup>	6	OCH <sub>3</sub>
H <sub>D50</sub>								
→4)-β-Xylp(1→	4.38	3.19	3.46	3.70	3.31	4.03		
	101.6	72.7	73.5	76.3	62.9	62.9		
α-GlcAp-(1→2	5.32	3.38	3.71	3.13	4.15			3.37
	99.8	70.9	71.3	82.3	71.2		173.2	59.9
α-Araf-(1→3	5.40	4.08	3.90	4.23	3.73	3.76		
	107.3	80.4	76.1	84.7	60.5	60.5		
→4)-β-Xylp(1→, 3-O-Ac	4.48		4.61					
	101.5		73.2					
→4)-β-Xylp(1→, 2-O-Ac	4.61	4.90						
	100.0	74.9						
H <sub>D80</sub>								
→4)-β-Xylp(1→	4.39	3.19	3.46	3.29	3.28	4.03		
	101.6	72.7	73.6	76.3	62.9	62.9		
α-GlcAp-(1→2	5.31	3.52	3.73	3.15	4.19			3.38
	99.6	71.5	71.2	82.4	71.9		171.1	59.9
α-Araf-(1→3	5.31	4.07	3.85	4.20	3.72	3.76		
	107.6	80.8	77.1	84.7	60.5	60.5		

<sup>a</sup>ax = axial. <sup>b</sup>eq = equatorial.

average molecular weights of the hemicellulosic subfractions decreased. FT-IR and NMR analysis indicated that the highly acetylated hemicelluloses precipitated at the relatively lower concentration of saturated ammonium sulfate (50%), and thus the gradient ammonium sulfate technique could discriminate acetyl and non-acetyl hemicelluloses. The DMSO-soluble hemicellulosic subfraction H<sub>D50</sub> precipitated by 50% saturated ammonium sulfate mainly consists of poorly substituted O-acetyl arabino-4-O-methylglucurono-(1→4)-β-D-xylan, in which 4-O-Me-α-D-GlcA-(1→2) units was linked at position O-2, Araf residues at O-3, and O-acetyl groups at O-2 or O-3. The DMSO-soluble hemicellulosic subfraction H<sub>D80</sub> precipitated by 80% saturated ammonium sulfate is mainly composed of highly substituted arabino-4-O-methylglucuronoxylan and β-D-glucan.

## AUTHOR INFORMATION

### Corresponding Author

\*E-mail: rcsun3@bjfu.edu.cn. Tel: +86-10-62336903. Fax: +86-10-62336903.

### Notes

The authors declare no competing financial interest.

## ACKNOWLEDGMENTS

This work was supported by grants from the Beijing Forestry University Young Scientist Fund (2010BLX04), the Ministry of Science and Technology (973 project, 2010CB732204), the Natural Science Foundation of China (No. 30930073), the Fundamental Research Funds for the Central Universities (NO.YX2011-37), and the State Key Laboratory of Pulp and Paper Engineering (201029).

## REFERENCES

- Jeguirim, M.; Trouve, G. Pyrolysis characteristics and kinetics of *Arundo donax* using thermogravimetric analysis. *Bioresour. Technol.* **2009**, *100*, 4026–4031.
- Venendaal, R.; Jorgensen, U.; Foster, C. A. European energy crops: a synthesis. *Biomass Bioenerg.* **1997**, *13*, 147–185.

- Hanegraaf, M.; Biewinga, C.; Gert van der Bijl, E. Assessing the ecological and economic sustainability of energy crops. *Biomass Bioenerg.* **1998**, *15*, 345–355.

- Angelini, L. G.; Ceccarini, L.; Nassi, N.; Bonari, E. Comparison of *Arundo donax* L. and *Miscanthus x giganteus* in a long-term field experiment in Central Italy: analysis of productive characteristics and energy balance. *Biomass Bioenerg.* **2009**, *33*, 635–643.

- Angelini, L. G.; Ceccarini, L.; Bonari, E. Biomass yield and energy balance of giant reed (*Arundo donax* L.) cropped in central Italy as related to different management practices. *Eur. J. Agronom.* **2005**, *22*, 375–389.

- Faix, O.; Meier, D.; Beinhoff, O. Analysis of lignocelluloses and lignins from *Arundo donax* L. and *Miscanthus sinensis* Anderss. and hydrolyquefaction of *Miscanthus*. *Biomass* **1989**, *18*, 109–126.

- Neto, C. P.; Seca, A.; Nunes, A. M.; Coimbra, M. A.; Domingues, F.; Evtuguin, D.; Silvestre, A.; Cavaleiro, J. A. S. Variations in chemical composition and structure of macromolecular components in different morphological regions and maturity stages of *Arundo donax*. *Ind. Crop. Prod.* **1997**, *6*, 51–58.

- Sun, X. F.; Sun, R. C.; Fowler, P.; Baird, M. S. Extraction and characterization of original lignin and hemicelluloses from wheat straw. *J. Agric. Food Chem.* **2005**, *53*, 860–870.

- Wen, J. L.; Sun, Y. C.; Xu, F.; Sun, R. C. Fractional isolation and chemical structure of hemicellulosic polymers obtained from *Bambusa rigida* species. *J. Agric. Food Chem.* **2010**, *58*, 11372–11383.

- Theander, O.; Westerlund, E.; 1993. Quantitative analysis of cell wall components. In *Forage Cell Wall Structure and Digestibility*; Jung, H. G., Buxton, D. R., Hatfield, R. D., Ralph, J., Eds.; ASA/CSSA/SSSA: Madison, WI, 1993; pp 83–104.

- Shatalov, A. A.; Pereira, H. *Arundo donax* L. reed: New perspectives for pulping and bleaching. 5. Ozone-based TCF bleaching of organosolv pulps. *Bioresour. Technol.* **2008**, *99*, 472–478.

- Spencer, D. F.; Liow, P.; Chan, W. K.; Ksander, G. G.; Getsinger, K. D. Estimating *Arundo donax* shoot biomass. *Aquat. Bot.* **2006**, *84*, 272–276.

- Joseleau, J. P.; Barnoud, F. Hemicelluloses of young internodes of *Arundo Donax*. *Photochemistry* **1974**, *13*, 1155–1158.

- Seca, A. M. L.; Jose, J. A. S.; Cavaleiro, J. A. S.; Domingues, F. M. J.; Silvestre, A. G. D.; Evtuguin, D.; Neto, C. P. Structural characterization of the lignin from the nodes and internodes of *Arundo donax* Reed. *J. Agric. Food Chem.* **2000**, *48*, 817–824.



- (15) Glasser, W. G.; Kaar, W. E.; Jain, R. K.; Sealey, J. E. Separation, characterization and hydrogel-formation of hemicellulose from aspen wood. *Carbohydr. Polym.* **2000**, *43*, 367–374.
- (16) Canilha, L.; Silva, J. B. A. E.; Felipe, M. G.; Carvalho, W. Batch xylitol production from wheat straw hemicellulosic hydrolysate using *Candida guilliermondii* in a stirred tank reactor. *Biotechnol. Lett.* **2003**, *25*, 1811–1814.
- (17) Lloyd, L. L.; Kennedy, J. F.; Methacanon, P.; Paterson, M.; Knill, C. J. Carbohydrate polymers as wound management aids. *Carbohydr. Polym.* **1998**, *37*, 315–322.
- (18) Mirafteb, M.; Qiao, Q.; Kennedy, J. F.; Anand, S. C.; Grocock, M. R. Fibres for wound dressings based on mixed carbohydrate polymer fibres. *Carbohydr. Polym.* **2003**, *53*, 225–231.
- (19) Proksch, A.; Wagner, H. Structure analysis of a 4-O-methylglucuronarabinoxylan with immuno-stimulating activity from *Echinacea purpurea*. *Phytochemistry* **1987**, *26*, 1989–1993.
- (20) Yamada, H.; Nagai, T.; Cyong, J. C.; Otsuka, Y. Relationship between chemical structure and anti-complementary activity of plant polysaccharides. *Carbohydr. Res.* **1985**, *144*, 101–110.
- (21) Ebringerova, A.; Hromadkova, Z.; Hribalova, V. Structure and mitogenic activities of corn cob heteroxylans. *Int. J. Biol. Macromol.* **1995**, *17*, 327–331.
- (22) Sun, R. C.; Fang, J. M.; Tomkinson, J. Characterization and esterification of hemicelluloses from rye straw. *J. Agric. Food Chem.* **2000**, *18*, 1247–1252.
- (23) Buchala, A. J.; Fraser, C. G.; Wilkie, K. C. B. Quantitative studies on polysaccharides in non-endospermic tissues of oat plant in relation to growth. *Phytochemistry* **1971**, *10*, 1285–1288.
- (24) Fang, J. M.; Sun, R. C.; Fowler, P.; Tomkinson, J.; Hill, C. A. S. Esterification of wheat straw hemicelluloses in the *N,N*-dimethylformamide/lithium chloride homogeneous system. *J. Appl. Polym. Sci.* **1999**, *74*, 2301–2311.
- (25) Fang, J. M.; Sun, R. C.; Tomkinson, J.; Fowler, P. Acetylation of wheat straw hemicellulose B in a new non-aqueous swelling system. *Carbohydr. Polym.* **2000**, *41*, 379–387.
- (26) Peng, F.; Ren, J. L.; Xu, F.; Bian, J.; Peng, P.; Sun, R. C. Comparative study of hemicelluloses obtained by graded precipitation from sugarcane bagasse. *J. Agric. Food Chem.* **2009**, *57*, 6305–6317.
- (27) Peng, F.; Ren, J. L.; Xu, F.; Bian, J.; Peng, P.; Sun, R. C. Fractionation of alkali-solubilized hemicelluloses from delignified *Populus gansuensis*: structure and properties. *J. Agric. Food Chem.* **2010**, *58*, 5743–5750.
- (28) Peng, F.; Ren, J. L.; Xu, F.; Bian, J.; Peng, P.; Sun, R. C. Comparative studies on the physico-chemical properties of hemicelluloses obtained by DEAE-cellulose-52 chromatography from sugarcane bagasse. *Food Res. Int.* **2010**, *43*, 683–693.
- (29) Stec, J.; Bicka, L.; Kuzmak, J. Isolation and purification of polyclonal IgG antibodies from bovine serum by high performance liquid chromatography. *Bull. Vet. Inst. Pulawy.* **2004**, *48*, 321–327.
- (30) Buchala, A. J.; Fraser, C. G.; Wilkie, K. C. B. Quantitative studies on polysaccharides in non-endospermic tissues of oat plant in relation to growth. *Phytochemistry* **1971**, *10*, 1285–1288.
- (31) Xu, F.; Geng, Z. C.; Sun, J. X.; Liu, C. F.; Ren, J. L.; Sun, R. C.; Fowler, P.; Baird, M. S. Fractional and structural characterization of hemicelluloses from perennial ryegrass (*Lolium perenne*) and cocksfoot grass (*Dactylis glomerata*). *Carbohydr. Res.* **2006**, *341*, 2073–2082.
- (32) Meakawa, E. Studies on hemicelluloses of bamboo. *Wood Res.* **1976**, *59/60*, 153–176.
- (33) Chaikumpollert, O.; Methacanon, P.; Suchiva, K. Structural elucidation of hemicelluloses from Vetiver grass. *Carbohydr. Polym.* **2004**, *57*, 191–196.
- (34) Smith, B. J.; Harris, P. J. The polysaccharide composition of Poales cell walls: Poaceae cell walls are not unique. *Biochem. Systemat. Ecol.* **1999**, *27*, 33–53.
- (35) Wedig, C. L.; Jaster, E. H.; Moore, K. J. H. Hemicellulose monosaccharide composition and in vitro disappearance of prchard grass and alfalfa hay. *J. Agric. Food Chem.* **1987**, *35*, 214–218.
- (36) Izydorczyk, M. S.; Biliaderis, C. G. Studies on the structure of wheat-endosperm arabinoxylans. *Carbohydr. Polym.* **1994**, *24*, 61–71.
- (37) Hoffmann, R. A.; Roza, M.; Maat, J. Structural characteristics of the cold-water-soluble arabinoxylans from the wheat flour of the soft wheat variety kadet. *Carbohydr. Polym.* **1991**, *15*, 415–430.
- (38) Izydorczyk, M. S.; Biliaderis, C. G. Influence of structure on the physicochemical properties of wheat arabinoxylan. *Carbohydr. Polym.* **1992**, *17*, 237–247.
- (39) Gruppen, H.; Hamer, R. J.; Voragen, A. G. J. Water-unextractable cell wall material from wheat 2. fraction of alkali-extracted polymers and comparison with water-extractable arabinoxylans. *J. Cereal Sci.* **1992**, *13*, 53–67.
- (40) Kacurakova, M.; Ebringerova, A.; Hirsch, J.; Hromadkova, Z. Infrared study of arabinoxylans. *J. Sci. Food Agric.* **1994**, *66*, 423–427.
- (41) Mathew, M. D.; Jain, A. K.; Ray, P. K. Infrared-spectra of Jute. *Cell Chem. Technol.* **1987**, *21*, 17–29.
- (42) Sjöström, E. Wood polysaccharides. In *Wood Chemistry, Fundamentals and Applications*; Sjöström, E., Ed.; Academic Press: New York, 1981; pp 61–67.
- (43) Sandula, J.; Kogan, G.; Kacurakova, M.; Machova, E. Microbial (1→3)- $\beta$ -D-glucans, their preparation, physico-chemical characterization and immunomodulatory activity. *Carbohydr. Polym.* **1999**, *38*, 247–253.
- (44) Chatjigakisa, A. K.; Pappasa, C.; Proxeniab, N.; Kalantzib, O.; Rodisb, P.; Polissioua, M. FT-IR spectroscopic determination of the degree of esterification of cell wall pectins from stored peaches and correlation to textural changes. *Carbohydr. Polym.* **1998**, *37*, 395–408.
- (45) Marchessault, R. H.; Liang, C. Y. The infrared spectra of crystalline polysaccharides. VIII. Xylans. *J. Polym. Sci.* **1962**, *59*, 357–378.
- (46) Vazquez, G.; Antorrena, G.; Gonzalez, J.; Freire, S. FTIR, H-1 and C-13 NMR characterization of acetosolv-solubilized pine and eucalyptus lignins. *Holzforchung* **1997**, *51*, 158–166.
- (47) Hoffmann, R. A.; Kamerling, J. P.; Vliegthart, J. F. G. Structural features of a water-soluble arabinoxylan from the endosperm of wheat. *Carbohydr. Res.* **1992**, *226*, 303–311.
- (48) Ohkoshi, M.; Kato, A.; Hayashi, N. C-13-NMR analysis of acetyl groups in acetylated wood. 1. Acetyl groups in cellulose and hemicellulose. *Mokuzai Gakkaishi* **1997**, *43*, 327–336.
- (49) Teleman, A.; Lundqvist, J.; Tjerneld, F.; Stalbrand, H.; Dahlman, O. Characterization of acetylated 4-O-methylglucuronoxylan isolated from aspen employing  $^1\text{H}$  and  $^{13}\text{C}$  NMR spectroscopy. *Carbohydr. Res.* **2000**, *329*, 807–815.
- (50) Teleman, A.; Tenkanen, M.; Jacobs, D. O. Characterization of O-acetyl-(4-O-methylglucurono)xylan isolated from birch and beech. *Carbohydr. Res.* **2002**, *337*, 373–377.
- (51) Roubroeks, J. P.; Andersson, R.; Aman, P. Structural features of (1→3), (1→4)- $\beta$ -D-glucan and arabinoxylan fractions isolated from rye bran. *Carbohydr. Polym.* **2000**, *42*, 3–11.
- (52) Wen, J. L.; Sun, Y. C.; Xu, F.; Sun, R. C. Fractional isolation and chemical structure of hemicellulosic polymer obtained from *Bambusa rigida* species. *J. Agric. Food Chem.* **2010**, *58*, 11372–11383.